Asynchronous formation of Hesperian and Amazonian-aged deltas on Mars and implications for climate

E. Hauber,[1] T. Platz,[2] D. Reiss,[3] L. Le Deit,[1] M. G. Kleinhans,[4] W. A. Marra,[4] T. de Haas,[4] and P. Carbonneau[5]

[1]   Most fluvial and lacustrine landforms on Mars are thought to be old and have formed more than ~3.8 Gyr ago, in the Noachian period. After a major climatic transition, surface liquid water became less abundant and finally disappeared almost completely. Recent work has shown that observational evidence for Hesperian and Amazonian aqueous processes is more common than previously recognized, but their nature is poorly understood. Moreover, it is not clear how the paleoclimate of Mars can be constrained by this activity. Here we report our investigation of a population of deltas around the ancient impact basin Chryse Planitia. To test whether the results are globally applicable, we also studied selected deltas with similar morphologies in the eastern hemisphere and found that the results are consistent. We compared the morphology of deltas, feeder channels, and receiving lakes, dated deltas by crater counting and searched for alteration minerals in hyperspectral images. The valleys and associated late-stage deltas were formed by short-lived aqueous processes, as suggested by their morphology and the general lack of associated aqueous alteration minerals. The likely source of water was neither widespread precipitation nor a regionally connected groundwater aquifer, but water mobilized locally from the cryosphere. Delta formation in our study areas occurred from the Early Hesperian to the Late Amazonian and did not require sustained periods of global climatic conditions favoring widespread precipitation. Liquid surface water has been locally present on Mars even after the Noachian, although only episodically, for transient intervals, and widely separated in space.

1.   Introduction

[2]   Geomorphological and mineralogical evidence suggests that liquid water was once present at and near the surface of Mars [e.g., *Baker*, 2001; *Bibring et al.*, 2006]. Widespread and numerous exposures of phyllosilicate-bearing material in the ancient southern highlands [*Poulet et al.*, 2005; *Ehlmann et al.*, 2013] point toward globally distributed water in the Noachian period (the Noachian is the oldest of Martian chronostratigraphic systems and ends, model dependent, sometime between ~3.74 and 3.57 Gyr ago) [*Werner and Tanaka*, 2011]). Phyllosilicates are rare in terrains younger than the Noachian, i.e., in regions of Hesperian (ending at ~3.5 to 3 Ga) and Amazonian (up to present) age, which display aqueous alteration minerals that are dominated by sulfates [*Gendrin et al.*, 2005]. The analysis of fluvial geomorphology supports the view that the Noachian was the period when surface water was most abundant, although the duration and intensity of fluvial processes in the Noachian are still unknown. An early period of intense degradation with relatively high erosion rates [*Golombek et al.*, 2006] has left a record of degraded craters [*Craddock and Maxwell*, 1993; *Craddock et al.*, 1997], but there are few directly observable traces of fluvial processes that may have caused this degradation. For example, no large, integrated drainage basins were formed at that time [*Aharonson et al.*, 2002; *Stepinski and Coradetti*, 2004; *Grant and Parker*, 2002]. Most valley networks, the strongest morphological indicators for widespread water on early Mars, were only formed later in the late Noachian and early Hesperian [*Fassett and Head*, 2008a; *Hoke and Hynek*, 2009], perhaps during a period of more intensive fluvial dissection associated with a climate optimum [*Irwin et al.*, 2005; *Howard et al.*, 2005]. Although the valley networks are widely interpreted as evidence for a relatively warmer and wetter climate during the Noachian as compared today, it is a matter of ongoing debate how warm and wet this period

---

was. Some characteristics of the valley networks, such as their relatively low drainage densities [*Stepinski and Coradetti*, 2004; *Luo and Stepinski*, 2006; *Hynek et al.*, 2010; *Erkeling et al.*, 2010] and other morphometric properties, e.g., a paucity of crater rim exit breaches or the shape of longitudinal valley profiles [e.g., *Barnhart et al.*, 2009; *Penido et al.*, 2013], suggest that Martian valley networks are immature as compared to terrestrial drainage patterns and do not indicate an Earth-like climate on Mars that would have been sustained over prolonged periods of time (reviews by *Irwin et al.* [2008] and *Carr* [2012]). There is also no consensus on the relative roles of surface water versus groundwater in valley formation [e.g., *Craddock and Howard*, 2002; *Goldspiel and Squyres*, 2000].

[3] After the Noachian/Hesperian boundary, much surface evidence suggests that the intensity of fluvial activity has decreased since. Evidence for liquid surface water is much less abundant than for the Noachian period, and it has been proposed that the relative importance of groundwater increased [e.g., *Harrison and Grimm*, 2005; *Andrews-Hanna et al.*, 2007; *Andrews-Hanna and Lewis*, 2011]. Although some dendritic valley networks were formed in the Hesperian [*Mangold et al.*, 2004] and even in the Amazonian, they are less numerous than in the Noachian and are restricted to some plateaus and the flanks of volcanoes [e.g., *Gulick and Baker*, 1990]. It has been suggested that post-Noachian valleys in Martian midlatitudes may be related to the melting of snow and/or ice and subsequent runoff [*Fassett and Head*, 2007; *Fassett et al.*, 2010; *Howard and Moore*, 2011] or to localized events such as melting of ground ice by the emplacement of hot impact ejecta or a transient climate episode [*Mangold et al.*, 2012]. The (late) Hesperian and the early Amazonian have also been the times when giant outflow channels were carved into the Martian surface by catastrophic flooding events [*Baker and Milton*, 1974]. The water eroding the channels would have flowed toward the northern lowlands where it may have formed transient oceans, inducing climate excursions and precipitation [*Baker et al.*, 1991]. Since the outflow channels start full sized at zones of collapse (chaotic terrains), large amounts of water would have been required from the subsurface. In some cases, the sources of outflow channels are clearly linked to zones of tectonic activity (e.g., Mangala Vallis), and it has been hypothesized that a confining cryosphere has been cracked by dikes [*Head et al.*, 2003; *Wilson and Head*, 2004], quickly releasing large amounts of water from an underlying pressurized aquifer [e.g., *Carr*, 1979; *Clifford*, 1993; *Andrews-Hanna and Phillips*, 2007]. Importantly, the formation of outflow channels as envisaged by these authors not only permits but implies a cold Martian environment, since the cryosphere has to be thick enough (>1 km [*Carr*, 1979]) to confine an aquifer with the required superlithostatic pressures to generate the large water volumes.

[4] Toward the late Amazonian, fluvial activity decreased even more and the only well-documented traces are the so-called gullies [*Malin and Edgett*, 2000], which are a few million years old or even younger [*Reiss et al.*, 2004; *Schon et al.*, 2009]. Although their origin is still under debate, a formation by drainage from aquifers seems unlikely [*Dickson and Head*, 2009; *Reiss et al.*, 2009]. Instead, the source of water may have been melting snow or ice [e.g.,

Costard et al., 2002; *Christensen*, 2003; *Williams et al.*, 2009; *Hauber et al.*, 2011]. Very high resolution repeat images of the Martian surface have revealed that some possibly aqueous activity still persists even at present. Changes in gullies have been attributed to water [*Reiss et al.*, 2010], although dry transport processes involving seasonally accumulated CO_2 were proposed alternatively [*Dundas et al.*, 2012]. Transient liquid water, perhaps as brines with a lowered freezing point [*Möhlmann and Thomsen*, 2011], might also be responsible for the slow albedo changes that have been observed on equator-facing slopes in the southern hemisphere during summer [*McEwen et al.*, 2011]. These recurrent albedo changes, termed recurrent slope lineae, propagate downslope with a speed of up to 20 m/d, resembling water flowing downward or wetting the ground if flowing in the shallow subsurface.

[5] In summary, there is a broad consensus based on mineralogical and geomorphological observations that after a more water-rich phase early in its history, Mars experienced a major climatic change at the Noachian/Hesperian boundary. After this change, the origin of which is still unknown [*Lammer et al.*, 2013], the planet approached its current cold and hyperarid state. There are, however, still many open questions concerning the aqueous history of post-Noachian Mars. For example, it is not clear whether the nature of aqueous processes was the same before and after this change, but perhaps different in intensity. How quickly did the amount of surface water decrease? Several lines of evidence suggest that it must have been fast, since the fresh preservation state of Hesperian landforms and the implied very low erosion rates [*Golombek et al.*, 2006], as well as the persistence in Hesperian terrains of minerals that are prone to aqueous weathering [*Tosca and Knoll*, 2009], strongly limit the amount of possible liquid water. But if liquid surface water had almost completely disappeared in the Hesperian, how will the water-related morphology of Hesperian and Amazonian surface features be explained? Can they all be linked to the release of water from aquifers confined beneath the cryosphere, such as the outflow channels? Is there a need to invoke transient periods of precipitation, perhaps dominated by snowfall, to explain fluvial features of Hesperian age [*Grant and Wilson*, 2011, 2012], or can they form under conditions close to the present ones?

[6] To address some of these questions, we revisited a part of Xanthe Terra where a number of fluvial valleys and channels and associated deltaic deposits can be observed [*Hauber et al.*, 2009]. Our main objective was to use newly available high-resolution data and determine whether the deltas (and, implicitly, lakes) indeed correspond to the period of intense fluvial activity more than ~3.8 Gyr ago, as it is the case for some deltas on Mars [e.g., *Fassett and Head*, 2005; *Ansan et al.*, 2011], or whether they are younger, as other Martian deltas and alluvial fans [*Cabrol and Grin*, 2001; *Grant and Wilson*, 2011]. We analyzed the morphology of deltas and associated valleys, determined their absolute model ages by crater counting, and searched for the spectral signatures of alteration minerals that might have formed in response to fluvial and/or lacustrine processes. To test whether our results apply only regionally (to Xanthe Terra), or perhaps globally, we also investigated similar deltas in the eastern hemisphere (i.e., Aeolis and Nephentes regions).

2. Data and Methods

[7] For morphologic interpretations, we relied on images acquired by CTX (Context Camera) [*Malin et al.*, 2007], HRSC (High Resolution Stereo Camera) [*Jaumann et al.*, 2007], and HiRISE (High Resolution Imaging Science Experiment) [*McEwen et al.*, 2007], with typical resolutions of 5–6, 10–20, and ~0.3 m/pixel, respectively. Topographic information was derived from MOLA (Mars Orbiter Laser Altimeter [*Zuber et al.*, 1992] Mission Experiment Gridded Data Records, with a cell size of ~460 m) for regional elevations and from HRSC gridded Digital Elevation Models (DEMs) for local analysis. HRSC DEMs are interpolated from 3-D points with an average intersection error of 12.6 m and have a regular grid spacing of 50 to 100 m [*Scholten et al.*, 2005; *Gwinner et al.*, 2010].

[8] Detailed determinations of observed crater populations formed on, within, and below deltaic surfaces are based on HiRISE, CTX, and Mars Orbiter Camera [*Malin et al.*, 1992] imagery. Raster data were stored in a geographic information system environment. Crater counts were performed with the ArcGIS software extension *CraterTools* [*Kneissl et al.*, 2011] and measured crater statistics were analyzed with the *craterstats* software [*Michael and Neukum*, 2010]. The crater size-frequency distribution (CSFD) of each counting area was analyzed for secondary or primary crater clusters using mean second closest neighbor distance and mean standard deviation of adjacent areas analyses [*Michael et al.*, 2012] which is implemented in *craterstats* [*Michael and Neukum*, 2010]. The identification of impact craters and counting areas as well as the derivation of absolute model ages and their interpretation is applied following the detailed description of *Platz et al.* [2013]. Absolute model ages were derived using the chronology and production functions of *Hartmann and Neukum* [2001] and *Ivanov* [2001], respectively. Since HiRISE images were partially used for CSFD determinations, craters up to 15 m in diameter were measured—the lower limit of the production function [*Ivanov*, 2001].

[9] We emphasize that distinguishing large impact craters exposed on the surface from those that formed on the underlying unit (i.e., crater floor) and embayed by fluvial deposits was not always unambiguous if only visible imagery is employed. Therefore, we also utilized HRSC DEM to measure delta thicknesses and compared the data to calculated theoretical crater rim heights based on morphometric data of *Garvin et al.* [2003]. If both values were similar, we interpreted the delta to have formed after to the formation of the impact crater and hence excluded the crater from the fit range to model the absolute age of delta formation. In addition, for some deltas, erosion, steep slopes, and heavy mantling altered crater preservation and identification. As a consequence, the mapped crater population may be less than would be expected resulting in a younger model age.

3. Geologic Setting

[10] Most deltas studied here are located in northern Xanthe Terra, part of the heavily cratered ancient highlands of Mars (Figure 1a). More specifically, the deltas are spread in a region bordered by the outflow channels, Maja Valles and Tiu Valles, to the west and east, respectively. Toward the north, Xanthe Terra is confined by the large degraded Chryse impact basin where Chryse Planitia represents the main portion of the basin floor [*Rotto and Tanaka*, 1995]. The topographic surface of the intercrater plains ranges from about +1000 m in the southern part to −1500 m in the northern part, with a gradual decrease toward Chryse Planitia. Two other deltas were found around Chryse Planitia and are located in southeastern Tempe Terra and in Margaritifer Terra (Figure 1).

[11] The deltas studied for comparison are located in the eastern hemisphere, in the Nephentes and Aeolis Mensae regions (Figure 1b). These areas near the Martian dichotomy are characterized by an erosional degradation of the dichotomy boundary that produces a distinct topographic scarp and numerous erosional outliers ("Zeugenberge" or Mensae) of the southern highlands, collectively called fretted terrain [*Sharp*, 1973]. Fine-grained sediment is widely spread in the entire area [*Irwin et al.*, 2004], which also hosts outcrops of the Medusae Fossae Formation. The deltas in the eastern hemisphere were selected on the basis of their morphological similarity to the circum-Chryse deltas. They share the same high degree of preservation, and they are also linked to the same type of upstream valleys. Thus, they are considered to form an adequate control group.

[12] In terms of geologic setting, the study areas in the western and eastern hemispheres are quite different. The only obvious common characteristic is the location near the global dichotomy boundary, the transition between the southern highlands and the northern lowlands [*Irwin et al.*, 2010]. The nature of this boundary, however, is quite different. While the boundary forms a distinct topographic step in the Nephentes and Aeolis Mensae regions, it continuously grades from the southern highlands of Xanthe Terra into the smooth plains of Chryse Planitia.

4. Observations and Interpretations

4.1. Morphology

[13] The studied deposits in Xanthe Terra are mostly located in impact craters at the terminations of deep valleys with steep walls, abrupt (amphitheater-like) headwalls and few tributaries (Figures 2, 3, 5, and 6). The length of the valleys is very diverse. In some cases (e.g., Sabrina Vallis, Nanedi, and Hypanis Valles), they can reach lengths of several hundred kilometers, whereas others are less than 10 km long. The valleys feeding the smaller deposits typically enter the craters from the south (Figure 2). They commonly start at and cut into intercrater plains, but in some cases, they are incised into crater ejecta.

[14] The characteristics of these valleys have often been interpreted as evidence for sapping [*Pieri*, 1980; *Harrison and Grimm*, 2005], i.e., the retrogressive incision of valleys induced through seepage erosion by groundwater. Morphologically analogous valleys have been described from the Colorado Plateau (USA), Hawaii (USA), and the Western Desert in Egypt [*Laity and Malin*, 1985; *Howard et al.*, 1988; *Luo et al.*, 1997]. It has been questioned whether sapping alone has the required transport capacity to remove debris from valley floors [*Lamb et al.*, 2006, 2008], or a combination of seepage weathering and fluvial runoff might explain the observed morphology [e.g., *Luo and Howard*, 2008].
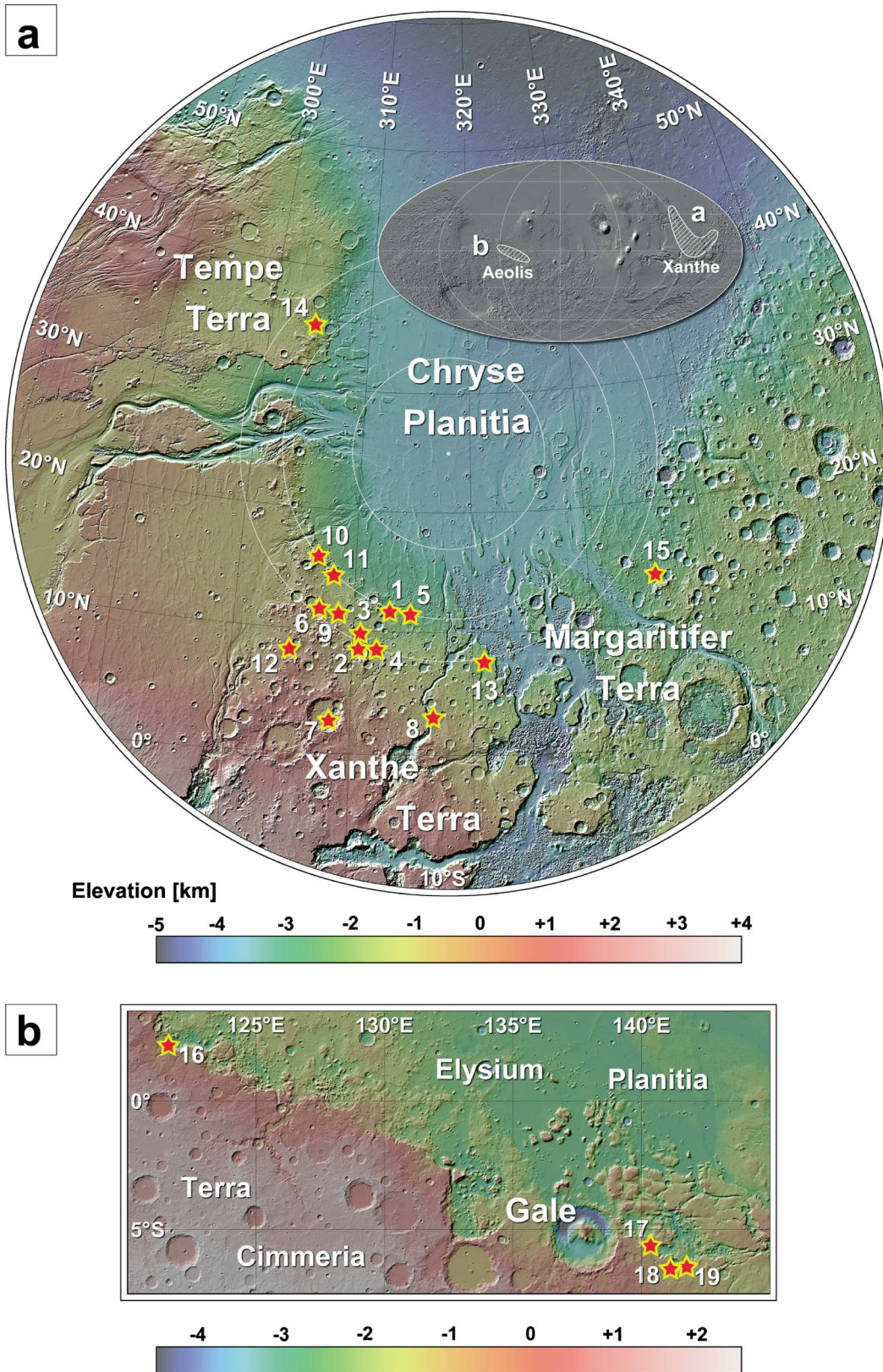
Figure 1. Context maps with delta locations marked by red asterisks (numbering corresponds to that used in Table 1). Background: color-coded elevations merged with shaded DEM, both based on MOLA data (inset shows locations in a global context). (a) Chryse Planitia in stereographic projection centered at 25° N/318°E [*Frey*, 2008]. In this projection, equal distances from the map projection center (i.e., Chryse Planitia) plot as circles (cf. Figure 8). (b) Eastern equatorial region between Terra Cimmeria and Elysium Planitia (Mercator projection).
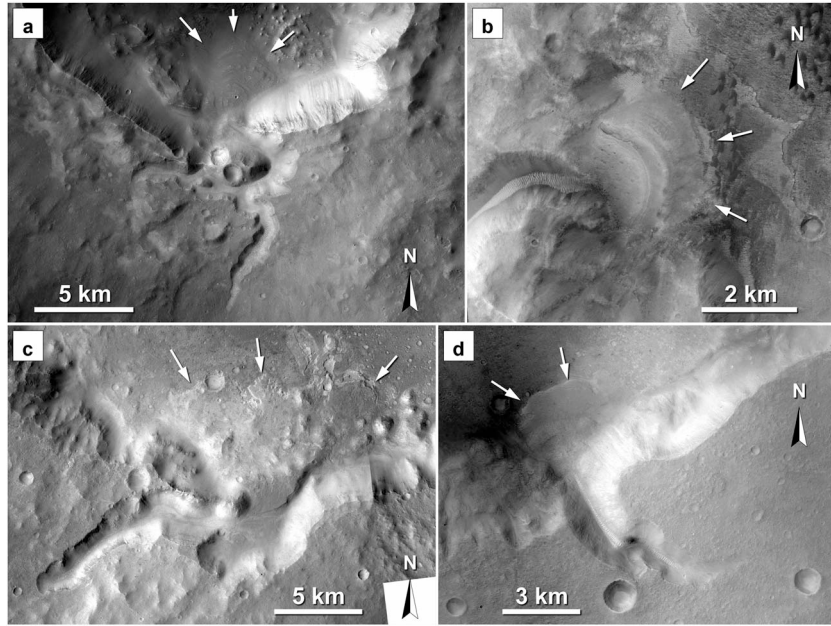
Figure 2. Newly observed deltas in Xanthe Terra and around Chryse Planitia (the examples shown here were not discussed in *Hauber et al.* [2009]). White arrows point to approximate front of delta. (a) Stepped delta in Balvicar crater (Xanthe Terra) at 16.04°N/306.78°E (#10 in Table 1 and Figure 1; detail of CTX image B21_017951_1995). (b) Gilbert-type delta with steep front in Kolonga Crater (Xanthe Terra) at 8.17°N/304.89°E (#12 in Table 1 and Figure 1; detail of CTX image B18_016804_1888). (c) Fan delta in Cantoura Crater (Xanthe Terra) at 14.52°N/308.17°E (#11 in Table 1 and Figure 1; detail of image mosaic from CTX images P16_007231_1927 and P20_008747_1923). (d) Delta or fan in unnamed crater north of Aram Chaos at 14.09°N/335.70°E (#15 in Table 1 and Figure 1; detail of CTX image B17_016460_1943).

[15] Morphologically, the deposits analyzed in this study resemble deltas more than alluvial fans. The latter are typically characterized by a conical shape with a constant slope or concave-upward geometry, and their distal margins grade smoothly into the adjacent plains [e.g., *Blair and McPherson*, 2009]. Alluvial fans on Mars display the same morphology [*Moore and Howard*, 2005]. On the other hand, the deposits studied here are markedly different. Their distal margin is clearly outlined by frontal scarps, with the single exception of the Hypanis deposits, which could be alluvial fans. Some distal scarps can be erosional (e.g., at the Sabrina delta) [*Hauber et al.*, 2009], but in most cases, they appear to be primary features, indicating a formation of the deposits as deltas. Moreover, the surfaces of the deposits do not show conical shapes, as expected for alluvial fans, but are rather flat. Overall, the morphology of the deposits suggests a formation as fan deltas. Some of the deposits display a remarkably well-preserved depositional morphology. A small fan delta in an unnamed crater in Xanthe Terra (Figure 3a) exhibits many meter-sized boulders at its surface. These boulders are spatially restricted to the delta surface and, therefore, are not ejecta from a nearby impact crater. Their flow mechanism must have been sufficiently energetic to transport this coarse material, and the elevation difference of >500 m from the upper rim of the feeder valley to the delta surface over a short lateral distance provides sufficient gravitational potential to explain such transport. The surface of a channel (Figure 3b) has a smoother texture, possibly indicating finer-grained material which may represent the final, less energetic stages of flow. Distinctive topographic scarps along the channel may be backward steps eroded in an upstream direction. Alternatively, they could be due to slightly more resistive layers in the deposit, perhaps as a result from sorting during deposition. The frontal scarp of the deposit displays pristine lobelike features (thin white arrows in Figure 3c), which we interpret as primary sedimentary lobes emplaced during fast deposition. A possible slump block (left) may indicate syndepositional deformation.

[16] Overall, this deposit does not appear much degraded. Additionally, other deposits in Xanthe Terra have a similar pristine morphology. Small deltas in Kolonga crater (Figure 2b) and at the terminus of Subur Vallis [see *Hauber et al.*, 2009, Figure 6] also seem to have experienced little modification. Displaying a flat top and a steep frontal scarp, their morphology strongly resembles that of Gilbert-type deltas [*Gilbert*, 1885, p. 106, Figure 4], which are characterized by coarse-grained sediments and typically prograde into deep basin margins (such as provided by an impact crater rim), forming a distinct architecture of flat-lying topsets, steeply dipping foresets, and flat or gently sloping bottomsets [*Nichols*, 2009]. Other observations support the notion of limited erosion of the Xanthe deltas (Figure 4a). For example, the delta at the mouth of Sabrina Vallis is similar in size as the well-studied Eberswalde delta (Figure 4b). The presence of exhumed and inverted distributary channels indicates that Eberswalde was degraded after the main depositional phase, most likely by deflation [e.g., *Wood*, 2006]. The Sabrina delta, in comparison, has eroded margins, but appears to be relatively pristine elsewhere, with a smooth upper surface and no traces of exhumed distributary
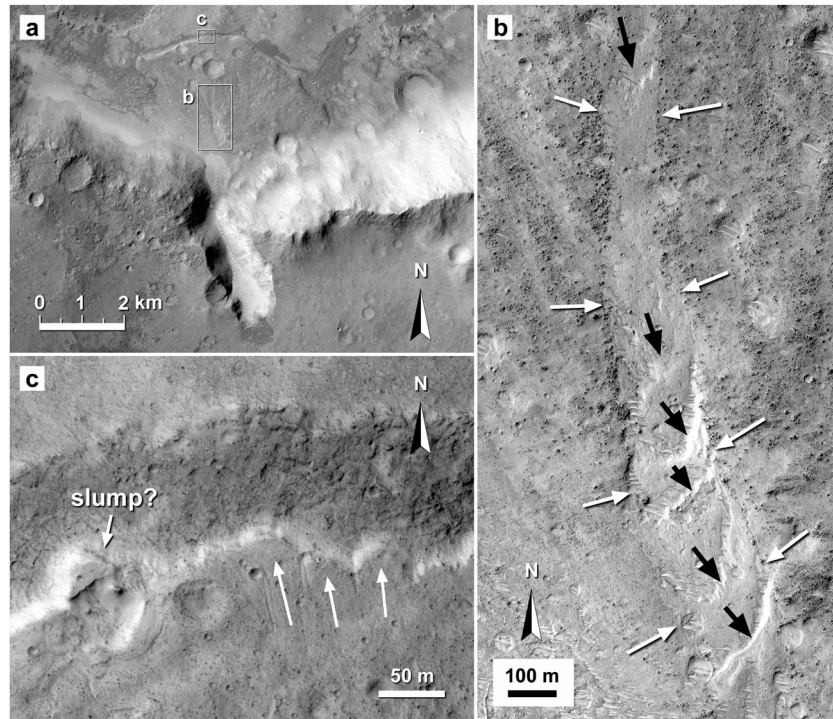
Figure 3. Small fan delta in unnamed crater in Xanthe Terra (at 11.38°N/308.72°E; #6 in Table 1 and Figure 1; detail of CTX image P20_008813_1911). (a) A very short valley cuts the flat floor of an older crater to the south and was the source of the material deposited in the delta. (b) Detail of delta surface with channel (outlines marked by white arrows). Detail of HiRISE image PSP_008813_1915. (c) Detail of delta front (detail of HiRISE image PSP_008813_1915).

channels. On the basis of this qualitative comparison and assuming that regional differences in erosion were not significant, therefore, the Sabrina delta appears to be younger than the Eberswalde delta, which is now thought to be early Hesperian in age [*Mangold et al.*, 2012]. The other deltas investigated in this study also do not exhibit exhumed and inverted channels on their surfaces, which are common elsewhere on Martian deltas and fans [*Pondrelli et al.*,

2008; *Williams et al.*, 2011; *Grant and Wilson*, 2012]. The limited degradation of most of the small deltas suggests that a significant fraction of the originally deposited volume is still present. Although their small sizes make a reliable determination of their volume and that of the valleys complicated, a qualitative comparison of delta and associated valley volumes suggests that they are quite similar (Figures 2, 3, 5, and 7). For example, the analysis of a HRSC DEM reveals
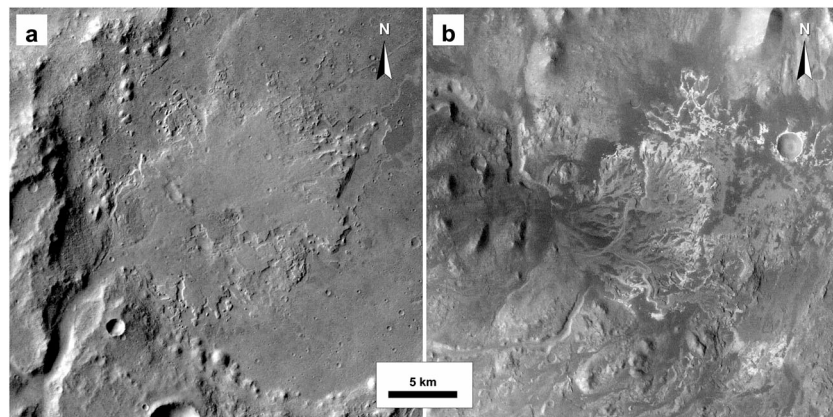
Figure 4. Comparison between the deposit at the terminus of Sabrina Vallis in Xanthe Terra and the Eberswalde delta. The Eberswalde delta is eroded and shows exhumed and inverted channels. The Sabrina delta has about the same size and appears to be less eroded, suggesting that it is younger than the Eberswalde delta. (a) Sabrina delta (#1 in Figure 1 and Table 1; detail of HRSC image h0894_0000; centered at 11.75°N/313.15°E). (b) Eberswalde delta (detail of HRSC image h2013_0000, centered at 23.85°S/326.75°E). North is up in both images.

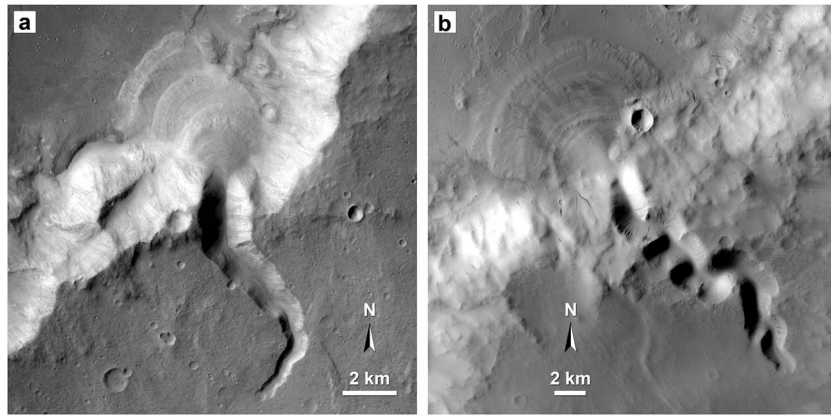**Figure 5.** A comparison between deltas in northern Xanthe Terra and Terra Sirenum. Both deltas display a "stepped" topography, which is thought to be indicative of a formation on very short timescales [*Kraal et al.*, 2008]. Note that in both cases, the deltas are fed from the south by short and deep valleys without tributaries. (a) Delta in Dukhan Crater (Xanthe Terra) at 7.59°S/321.03°E (#10 in Figure 1 and Table 1; detail of CTX image P02_001842_1714). (b) Delta in Terra Sirenum at 8.60°S/200.72°E, studied by *Kraal et al.* [2008] and by *Kleinhans et al.* [2010]. Detail of CTX image P02_001644_1713.

that the valley feeding the small delta shown in Figure 3 has an area of ~3.4 km^2 and a volume of ~0.15 km^3. The delta has a surface of about 10.6 km^2 and a thickness at its distal margin of less than 50 m. This thickness is certainly not uniform over the entire delta surface and may be expected to decrease toward the apex, since the delta is superposed on a sloping crater rim. Therefore, the delta volume is comparable to the valley volume. A similar relationship is observed for the delta #15 (Figure 2d), where the valley area and volume are 13.5 km^2 and ~1.5 km^3, respectively. With a delta surface area of 11.2 km^2, this volume would correspond to an average delta thickness of ~130 m. We observe delta thicknesses between ~50 and 150 m, which is in good agreement with the hypothesis that delta and valley volumes are very similar.

[17] Several deltas display morphologies that are indicative of short-lived processes. The delta in Dukhan Crater displays a terraced or stepped profile from its apex to the crater floor. Such morphology was observed elsewhere on Mars (e.g., in Terra Sirenum) and could only be reproduced with a single short outflow event in the laboratory and in a numerical model based on physics of flow and sediment transport [*Kraal et al.*, 2008; *Kleinhans et al.*, 2010; *de Villiers et al.*, 2013]. The deltas in Dukhan (Figure 5) and Balvicar (Figure 2a) craters are strikingly similar to the delta studied
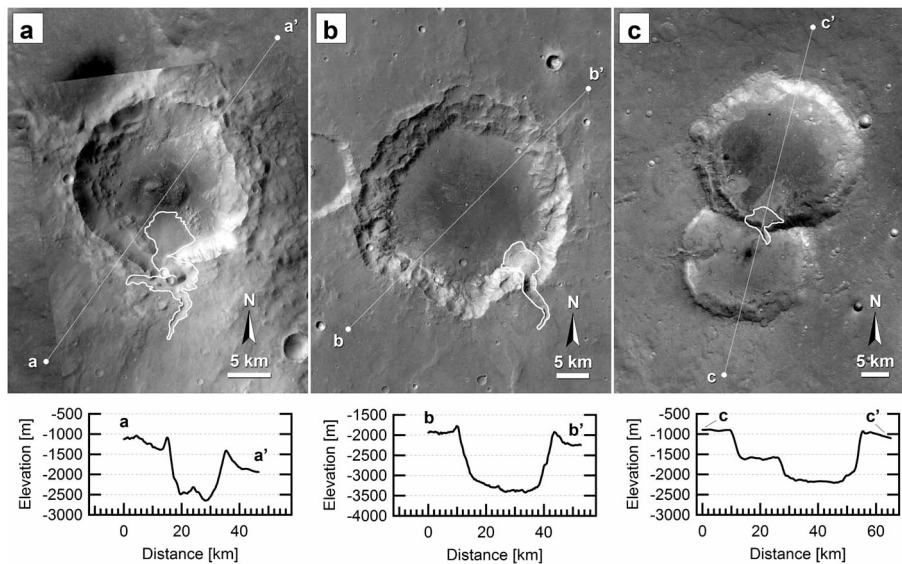
Figure 6. Topographic cross sections across craters hosting deltas in Xanthe Terra. The deltas and the associated feeder valleys are highlighted by white lines. Profiles were measured on DEM derived from HRSC stereo images. Scale and vertical exaggeration are the same for all profiles shown at the bottom of the figure. (a) Balvicar Crater (#9 in Table 1 and Figure 1; detail of CTX image B21_017951_1955 superposed on detail of HRSC image h2277_0000). (b) Dukhan Crater (#12 in Table 1 and Figure 1; detail of HRSC image h1187_0001). (c) Unnamed crater (#6 in Table 1 and Figure 1; detail of HRSC image h2244_0000).

Figure 7. Deltas in the Nephentes and Aeolis Mensae regions close to the dichotomy boundary in the eastern hemisphere of Mars. Note that just like in Xanthe Terra (cf. Figure 2), all deltas were fed by short and deep valleys without tributaries and a topographic gradient toward north. (a) Delta with steep frontal scarp in Aeolis Mensae region at 5.62°S/140.49°E (#17 in Table 1; detail of CTX image G12_022902_1742).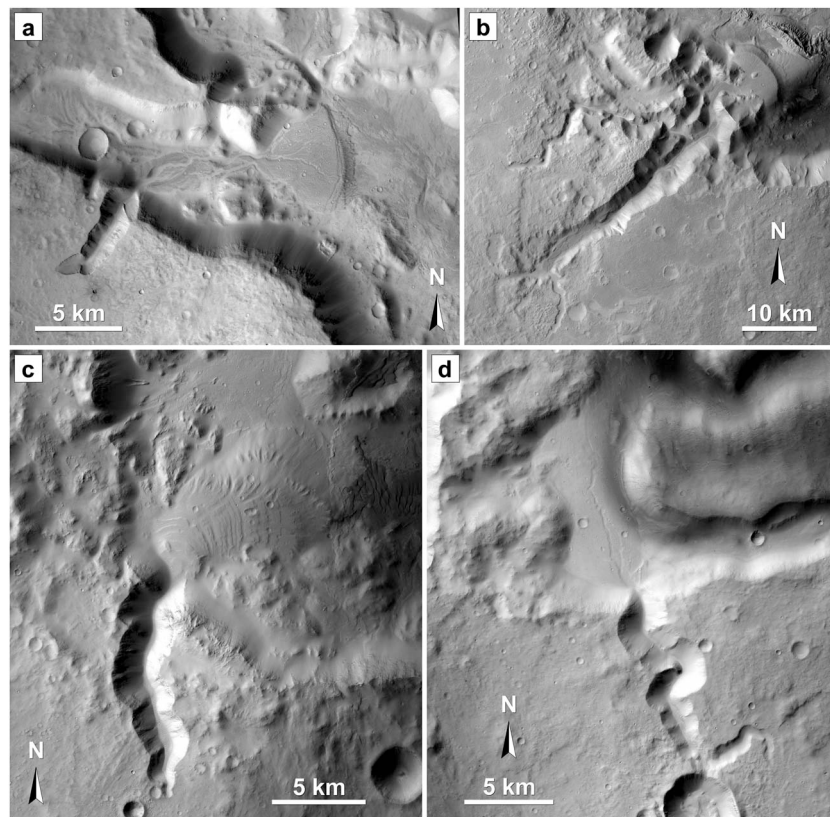 (b) Delta with steep frontal scarp in Nephentes Mensae region at 2.16°N/121.64°E (#16 in Table 1; detail of HRSC image h5212_0000). (c) Delta with multiple lobes or terraces in Aeolis Mensae region at 6.54°S/141.12°E (#18 in Table 1; detail of CTX image B01_009874_1735). (d) Fan delta in Aeolis Mensae region at 6.49°S/141.69°E (#19 in Table 1; detail of CTX image G20_026104_1735).

by *Kraal et al.* [2008] and may have been formed by comparably fast processes.

[18] The craters hosting the deltas show different morphologies. Some of them appear rather pristine and are not filled by later deposits, whereas others have heavily degraded rims and are filled by materials forming a flat, nearly homogeneous surface (Figure 6). The craters portrayed in Figure 6 show different stages of degradation and infilling. While the crater shown in Figure 6a has a relatively pristine profile with raised rims, a deep-lying crater floor, and a central peak, the middle crater (Figure 6b), although larger in diameter, is shallower and does not exhibit a central peak, which might have been buried by the infilling material. The shallow crater illustrated in Figure 6c is most degraded, without raised crater rim, and with a flat floor as a result of infilling processes. Obviously, the formation of deltas in craters did not depend on specific crater morphology. It has been shown recently that many craters on Mars with flat, infilled floors have been volcanically resurfaced over an extended period of time ranging from the late Noachian to the early Amazonian, with a peak resurfacing activity in the Hesperian [*Goudge et al.*, 2012b]. By inference, stratigraphic relationships

alone suggest that at least some deltas formed in the Hesperian after volcanic resurfacing.

[19] Most craters with deltas are closed basins, i.e., they do not have an outlet valley. Although more than 200 open-lake basins have been identified on Mars [*Fassett and Head*, 2008b; *Goudge et al.*, 2012a], most craters with deltas around Chryse Planitia are closed basins, i.e., they do not have an outlet valley. Only one delta appears to have formed in an open-lake basin (at the terminus of Nanedi Valles; delta #4 in Figure 1 and Table 1). Another deposit, at the terminus of Hypanis Valles (#5), is not formed in a crater but in a basin that would be defined by Chryse Planitia or, indeed, the entire northern lowlands. As already noted earlier [*Hauber et al.*, 2009, Figure 7], the morphology of this deposit resembles a fan more than a delta formed in a lake, not requiring a standing body of water in the northern lowlands. The other deposit not contained in a crater is the delta described by *Di Achille et al.* [2007], which is situated on the floor of the outflow channel, Shalbatana Vallis (#8). The delta at the end of Sabrina Vallis is hosted by a crater in which water would not pond to any significant height, but modeling by *Kleinhans et al.* [2010] showed that no ponding is needed to explain its morphology.

Table 1. Geographic Locations and Absolute Model Ages of Deltas[a]

#[b]	Delta Name[c]	Lat (°N)	Lon (°E)	Valley[d]	Valley Depth (m)[e]	Age (Ga)	+Error (Ga)	−Error (Ga)
				Xanthe, Tempe, and Margaritifer Terrae				
01	Sabrina	11.69	307.05	L	~150	3.43	0.11	0.35
02	Tyras	8.45	310.26	L	300–350	3.63[f]	0.05	0.08
03	Sibut	9.84	310.58	M	~200	n/a		
04	Nanedi	8.49	311.99	L	~100	3.60	0.08	0.16
05	Hypanis	11.3	314.57	L	~75 (?)	3.45	0.07	0.14
06	Subur	11.72	307.05	M	n/a	1.42	0.53	0.53
07	Camichel	2.74	308.33	M	~250	0.57	0.14	0.14
08	Shalbatana	3.05	316.75	M	~1100	3.35[g]	0.160	1.12
09	Unnamed	11.38	308.72	S	150	0.3	0.04	0.04
10	Balvicar	16.04	306.78	S	~300	0.84	0.17	0.17
11	Cantoura	14.52	308.17	S	600	1.95	0.55	0.56
12	Kolonga	8.17	304.89	S	~40 (?)	0.39	0.14	0.14
13	Dukhan	7.59	321.03	S	~250	0.29	0.055	0.055
14	Liberta	35.18	304.52	S	~50 (?)	0.84	0.19	0.19
15	Unnamed	14.09	335.70	S	500	0.92	0.53	0.53
				Eastern Hemisphere (Nephentes and Aeolis Mensae)				
16	Nephentes[h]	2.16	121.64	M	~820	1.80	0.48	0.48
17	Aeolis 1	−5.62	140.49	S	~350	0.99	0.094	0.094
18	Aeolis 2	−6.54	141.12	S	~600	3.46[i]	0.11	0.42
19	Aeolis 3	−6.49	141.69	S	400	0.47	0.06	0.06

[a]Full information about counting areas, crater size-frequency distributions, isochrones, and errors are provided in the supporting information.
[b]Corresponds to delta numbers in Figure 1.
[c]Name of crater or other landform hosting the delta.
[d]Length of feeder valley: L = long (>50 km), M = medium (15–50 km), S = short (<15 km).
[e]Measured in HRSC DEM near delta apex (question mark denotes large uncertainty).
[f]Three lobes have been dated on Tyras delta, with an age range from 3.35 (lower lobe) to 3.63 (upper lobe) Ga (the table gives the age for the upper lobe).
[g]Measured by *Di Achille et al.* [2007].
[h]See, e.g., *Kleinhans et al.* [2010].
[i]Three lobes have been dated on the Aeolis 2 delta, with an age range from 3.46 (lower lobe) to 0.4 (upper lobe) Ga (the table gives the age of the lower lobe).

[20] Overall, the deltas studied for comparison in the Nephentes and Aeolis Mensae regions are morphologically very similar to those around Chryse Planitia. They are also associated with short and deep valleys without tributaries (Figure 7), which drain from south to north. The deltas appear well preserved, as indicated by their unmodified surfaces and their pristine frontal scarps (e.g., Figures 7a and 7b). Some deltas (Figures 7a and 7d) display a simple geometry with a single deposit, a flat floor, and a distinct frontal scarp, which does not seem to be altered by postformation erosion. The delta in the Nephentes Mensae region (Figure 7b) is more complex and consists of two distinct lobes, and one of the deltas has a stepped or multilobate morphology (Figure 7c). The only obvious difference between the studied deltas in the eastern hemisphere and the Xanthe deltas is their location at the bottom of fretted valleys compared to impact craters in circum-Chryse deltas.

[21] The feeder valleys of the deltas are morphologically analogous to sapping valleys on Earth [*Laity and Malin*, 1985; *Howard et al.*, 1988] and, therefore, may suggest a subsurface source of the water. One possibility would be a regionally or even globally connected groundwater aquifer (such as proposed by, e.g., *Andrews-Hanna et al.* [2007]). This hypothesis would predict that the elevations of the deltas somehow reflect the groundwater table. A regional aquifer in Xanthe Terra would drain toward Chryse Planitia, which defines the regional base level. The elevations of the deltas, therefore, should increase with increasing distance from the center of Chryse Planitia. This hypothesis was tested by measuring the elevations of delta apices, distal margins, and valley source areas as well as their distance to

the center of Chryse Planitia as defined by *Frey* [2008] (25°N, 318°E). The three elevations were chosen to bracket the maximum range of possible groundwater elevation upon event initialization. No correlation between the distance to Chryse Planitia and the elevations of the deltas can be observed (Figure 8a). Hence, it is unlikely that the formation of the deltas was associated with a large, regionally connected groundwater aquifer. We note here that *Harrison and Grimm* [2009] for the time of outflow channel formation (late Hesperian/early Amazonian) and *Michalski et al.* [2013] for even earlier periods (early Hesperian and older) also argued against global-scale aquifers.

4.2. Presence of Alteration Minerals

[22] In order to investigate the presence of alteration minerals that may have formed in response to fluvial and/or lacustrine processes, we analyzed the CRISM (Compact Reconnaissance Imaging Spectrometer for Mars) [*Murchie et al.*, 2009] targeted observations (Targeted Reduced Data Record or TRDR) of deltas in Xanthe Terra and in the eastern hemisphere of Mars for comparison. Almost no alteration minerals have been detected on the investigated deltas so far, and only 3 of the 19 analyzed deltas appear to contain alteration minerals. This result suggests that the deltas are primarily composed of unaltered material. However, no CRISM TRDR observations were available for 6 of the 19 investigated deltas (#1, #2, #9–11, and #13 in Figure 1 and Table 1) at the time of manuscript submission. Moreover, most of the deltas are located in areas that have an intermediate Dust Cover Index (DCI) as defined by *Ruff and Christensen* [2002] using Thermal Emission Imaging System data. This suggests that the lack of alteration minerals may be explained by the
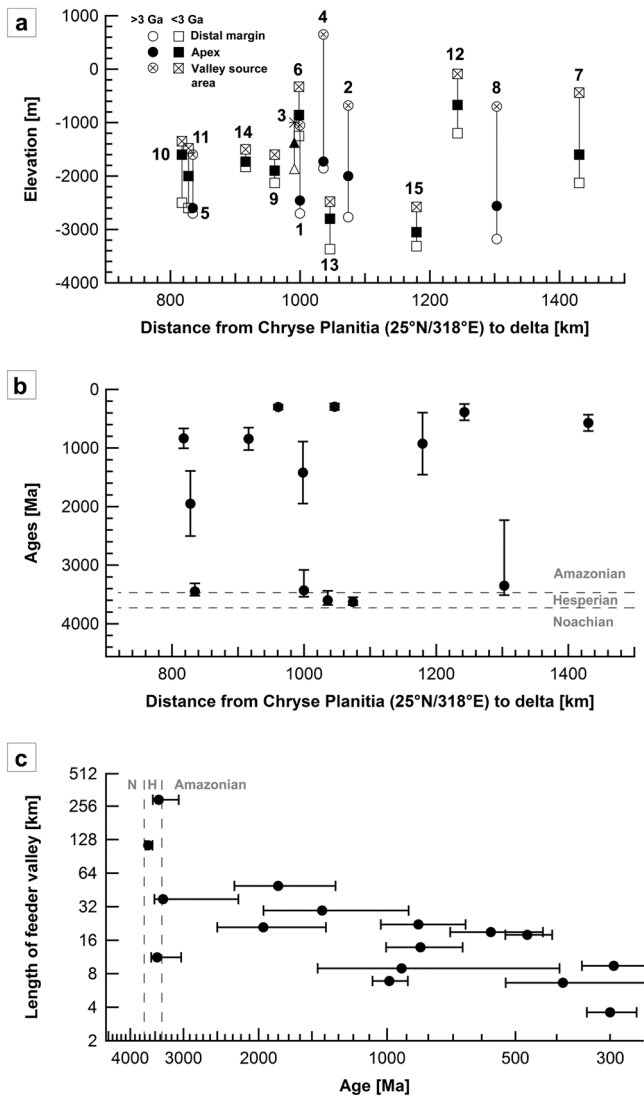
Figure 8. Delta properties as a function of their distance to the center to Chryse Planitia (at 25°N/318°E) [see *Frey*, 2008]. (a) Elevation of delta apices, distal margins, and source areas of feeder valleys. Numbers correspond to those used in Figure 1 and Table 1. Different symbol shapes were used to facilitate easy discrimination between older (>3 Ga; circles) and younger deltas (squares). (b) Ages of deltas. No correlation between ages and distances to Chryse Planitia can be observed. Note that the age of delta #3 in Sibut crater (triangles) could not be determined. (c) Lengths of feeder valleys versus ages. Note that the length of the Hypanis Valles (feeding delta #2) could not be determined due to later events [*Hauber et al.*, 2009] (N, Noachian; H, Hesperian).

presence of dust on the analyzed surfaces, which commonly prevents the underlying minerals to be observed by orbital imaging spectrometers. Nevertheless, three deltas (#7, #16, and #18 in Figure 1 and Table 1) for which we detected alteration minerals are all located in areas of intermediate to high DCI. Even though some deltas are likely covered by dust, the detection of potential alteration minerals is possible on localized dust-free areas. Additionally, no light-toned deposits, which are common geological landforms associated with alteration minerals as observed for, e.g., the phyllosilicates on the

plateaus surrounding Valles Marineris [*Le Deit et al.*, 2012], have been observed on HiRISE and CTX images of these deltas. Hence, the rare occurrence (or absence) of alteration minerals in the investigated delta is considered to be a true trend.

[23] The Amazonian-aged delta in Camichel crater (#7 in Figure 1 and Table 1) is the only delta investigated in Xanthe Terra which displays evidence of localized alteration. Some light-toned deposits on the distal part of the delta exhibit spectra with absorption bands at ~1.38 and ~1.9 μm, and a broad band between ~2.21 and ~2.26 μm that are consistent with opaline silica spectra [*Anderson and Wickersheim*, 1964; *Popa et al.*, 2010; *Carter et al.*, 2012] (Figure 9). Silica is a product of basaltic weathering, when water interacts with mafic rocks [*McLennan*, 2003], and has been found elsewhere on Mars [e.g., *Milliken et al.*, 2008]. The two other deltas containing alteration minerals are located in the eastern hemisphere. The 3.5 Gyr old fan delta Aeolis 2 (#18 in Table 1) contains opaline silica on its distal part (Figure 9). The Nephentes delta (#16 in Table 1) may also contain alteration phases such as opaline silica or phyllosilicates, but the analysis of the corresponding CRISM observations does not permit a reliable identification. These results are consistent with those of *Carter et al.* [2012], who showed that opal is the dominant hydrated mineral found in alluvial fans and deltas on Mars, followed by Fe/Mg clays.

[24] Our observations are consistent with previous studies showing that only few open-basin lake deposits contain alteration minerals on Mars [*Goudge et al.*, 2012a; *Carter et al.*, 2013]. This suggests that in situ alteration and precipitation is not a major process occurring in these paleolakes [*Goudge et al.*, 2012a]. Instead, the alteration minerals present in the lacustrine deposits likely correspond to transported materials reflecting the composition of the bedrock in their watersheds [*Mangold et al.*, 2007; *Dehouck et al.*, 2010; *Goudge et al.*, 2012a; *Carter et al.*, 2013]. The lack of in situ alteration may be explained by the short-lived lacustrine activity, and/or by environmental conditions not conducive to alteration [*Goudge et al.*, 2012a; *Carter et al.*, 2013]. The observation of opaline silica in fan deltas in Camichel and Aeolis 2 craters, as in other Martian craters [*Noe Dobrea et al.*, 2006; *Carter et al.*, 2013], is consistent with transient aqueous episodes. In the presence of water, opaline silica is sequentially transformed by diagenesis into opal-A, opal-CT, and microcrystalline quartz [*Williams et al.*, 1985; *Williams and Crerar*, 1985]. Therefore, opaline silica likely formed in situ during or shortly after the formation of the fan deltas [*Carter et al.*, 2012]. The presence of opaline silica shows that localized alteration took place on Mars even during the Amazonian, although water cannot have persisted for extended periods of time at these sites (see discussion by *Tosca and Knoll* [2009]).

4.3. Ages

[25] Model ages could be determined for all deltas except the delta in Sibut crater, where the degraded surface prevented the mapping of its extent (see supporting information). As a result, it was unclear whether larger craters were formed on the delta or next to it or whether those craters belong to the crater floor unit. For the Sabrina and the unnamed delta #15, a resurfacing age between 69 and
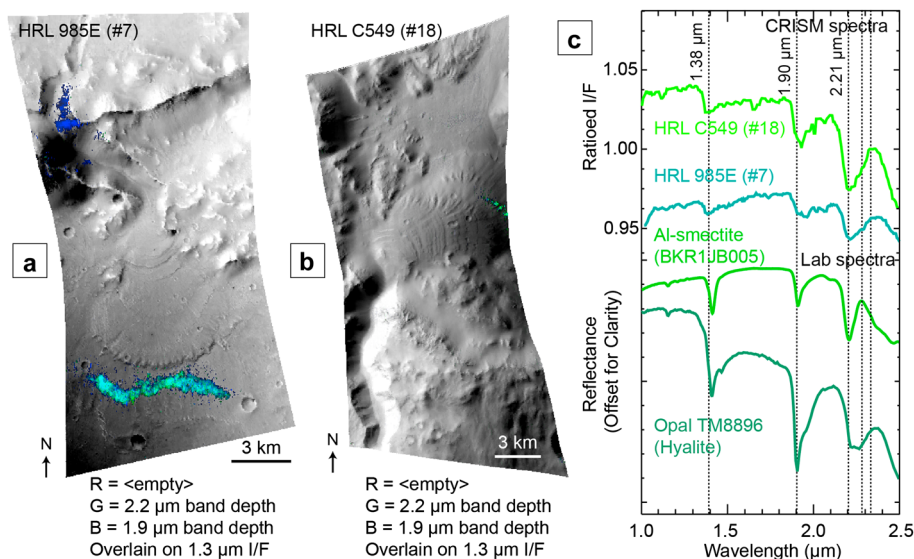
Figure 9. Opaline silica on the distal part of fan deltas in Xanthe Terra (Camichel, #7 in Table 1) and Aeolis Mensae (Aeolis 2, #18 in Table 1). (a) Band depth map (green, BD2200; blue, BD1900R) of the CRISM observation HRL 985E of Camichel at 2.71°N/308.34°E. Cyan tones indicate occurrence of opaline silica. (b) Similar band depth map of the CRISM observation HRL C549 of Aeolis 2 at 6.53°S/141.18°E. Green tones indicate occurrence of opaline silica. Colors in Figures 9a and 9b represent significant absorption band depths. (c) CRISM ratio spectra of opaline silica compared to laboratory spectra (RELAB spectral library) [*Clark et al.*, 2007].

77 Ma was determined representing delta modification by mantling deposits. Two model ages were also determined for the unnamed delta at location #9 and Aeolis 3. However, here the younger model age represents the delta formation age, whereas the older ages are derived from craters predating delta formation. The pristine morphology of unnamed delta #9 supports a young formation age of about 300 Ma (see supporting information). The old age of 3.52 Ga derived for the Aeolis 3 delta is only based on three craters, which are located at the delta periphery (i.e., only partially buried) and does not characterize the delta formation age. Although this delta is mantled by air fall deposits, the so-called resurfacing age of 469 Ma represents the delta formation age and is based upon a larger number of craters ranging in diameter from 60 to 200 m (see supporting information). The delta of Nanedi Valles is the only case where a formation age cannot be assigned with certainty. Since the delta occupies the entire small 6.5 km diameter crater, delta thickness could not have been determined (see supporting information). As a result, we were not able to distinguish whether the largest craters formed prior to or after delta formation. As a conservative approach, we used the older age of 3.60 Ga to be the age of delta formation.

[26] For Tyras and Aeolis 2 deltas, three model ages determined on distinct surfaces are reported and separated into upper, middle, and lower surfaces. Model ages reflect stratigraphic relations if their errors are also considered. The Tyras delta shows model ages between 3.35 and 3.63 Ga, whereas the Aeolis 2 delta reveals activity between 150–400 Ma and 3.46 Ga. The results of our crater counting study yield very diverse ages for the deltas in Xanthe Terra (Table 1 and supporting information). Although one delta may be as old as the late Noachian/early Hesperian transition (Tyras), by far most deltas appear to have formed in the Hesperian (3.37–3.71 Ga) and in the Amazonian (<3.37 Ga) [*Werner and Tanaka*, 2011; *Michael*, 2013]. The diverse results exclude a more or less synchronous formation at the Noachian/Hesperian boundary. The deltas in Nephentes and Aeolis Mensae, studied for comparison, have also diverse Hesperian and Amazonian ages (range: 3.52 to 0.98 Ga; Table 1), which overlap with those measured in Xanthe Terra. The results obtained in Xanthe Terra do not seem to be unique, therefore, and may be seen as global representatives for valleys and deltas that are morphologically analogous.

[27] We do not observe any correlation between delta age and distance to the center of Chryse Planitia (Figure 8b), which would be expected if delta formation were linked to a slowly rising or sinking groundwater table intersecting a gently sloping surface at different positions and elevations with time (Figure 8b). This supports the conclusions derived from delta and valley elevations and from their relationship to the outflow channels, i.e., their formation is not linked to a regional groundwater aquifer. Our results also imply that there is a correlation between delta ages and the lengths of their feeder valley. In general, it appears that the older deltas (>3 Ga) are linked to relatively long valleys, whereas younger deltas have shorter valleys (Figure 8c and Table 1).

5. Discussion

[28] The main objective of our study was the determination of absolute crater model ages of deltas in two study areas. Our results show that delta ages span a long time in Martian history, ranging from ~3.6 Ga (early Hesperian) to ~300 Ma (late Amazonian) (Table 1). The observation of a similar range of delta ages around Chryse Planitia and in the reference study area in the eastern hemisphere strongly

indicates that these results are globally applicable and that late-stage deltas are common on Mars. Independent studies of deltas with very similar morphological characteristics confirm this view [*Dehouck et al.*, 2010]. This age distribution is clearly not consistent with a formation of deltas within a short time interval under unique climatic conditions, such as has been proposed for valley network formation [*Howard et al.*, 2005; *Irwin et al.*, 2005]. This notion is not in contradiction to the conclusions of *Howard et al.* [2005] and *Irwin et al.* [2005], since we showed above that the deltas analyzed in this study are clearly not linked to the dendritic valley networks. The ages as determined by crater counting suggest a delta formation that corresponds to isolated events separated by long periods of quiescence. The climate in the late Hesperian and early Amazonian was on average already characterized by a low atmospheric pressure and corresponding dry and cold conditions [e.g., *Barabash et al.*, 2007; *Lammer et al.*, 2013]. Therefore, because the ages of the deltas correspond in time to this dry and cold period, mechanisms that could operate under these conditions are necessary to explain their formation. Lastly, our findings indicate that scenarios for delta formation should therefore not require spatially distributed rainfall.

[29] The morphology of the valleys linked to the deltas strongly suggests a major contribution of subsurface water and/or ice to flow generation, transport, and depositional processes. For example, although some surficial channels drain toward the abrupt heads of some of these valleys [*Hauber et al.*, 2009], the valleys lack a dendritic structure in plan view, which is commonly considered to be diagnostic of precipitation and overland runoff. In general, no converging pattern of tributaries to confluences can be observed. Moreover, the valleys typically start at distinct scarps and are relatively deep with respect to their lengths, which is atypical for dendritic valley networks. It has been suggested that the shape of such valleys is not necessarily indicative of sapping and can also be explained by erosion through layered stratigraphy or incision through a duricrust [*Howard et al.*, 2005], but the general lack of widespread fluvial dissection of the intercrater plains of Xanthe Terra argues against significant and distributed surface runoff such as required to form the dendritic valley networks. This conclusion is supported by the qualitative observation that the volumes of the smaller deltas and their associated valleys are similar. If true, this would argue against a significant contribution to delta volume by material eroded by overland runoff from interfluves on the plateaus surrounding the valleys, further supporting the notion that precipitation and runoff were not important factors in delta generation.

[30] The valley morphology in our study areas, therefore, does not support a dominant contribution of precipitation to the water supply and is consistent with the wide range of ages that indicates that valleys must have been able to form in cold and dry environments. Further support for a delta origin in cold conditions comes from theories of outflow channel formation. It is commonly assumed that they are formed by short-lived bursts of water originating in pressurized aquifers beneath a sealing cryosphere [e.g., *Carr*, 1979; *Hanna and Phillips*, 2005; *Andrews-Hanna and Phillips*, 2007]. To achieve the required pressure (commonly assumed to be superlithostatic [e.g., *Harrison and Grimm*, 2009]), the confining cryosphere has to be thick (>1 km [e.g.,

Andrews-Hanna and Phillips, 2007]), and thus the climate must have been cold. At least four of the studied deltas formed at times of outflow channel activity (~3.5 to 3 Ga) [e.g., *Tanaka et al.*, 2005; *Warner et al.*, 2009; *Lasue et al.*, 2013, and references therein], and most other studied deltas formed later. Hence, the cryosphere had a thickness of one kilometer or more when the older deltas formed, and it became even thicker during the formation of the younger deltas. Since the depths of the feeding valleys are typically much less than 1 km (Table 1), it follows that the water flowing in the valleys was likely derived from within the cryosphere. A water source for the deltas that is distinct from that of the outflow channels is also independently indicated by the lack of correlation between valley/delta elevations and the distance to Chryse Planitia (Figure 8a). If the valleys and deltas were fed by sapping from a subcryospheric aquifer, with a water table tracing the regional slope and draining toward Chryse Planitia (i.e., the regional base level), we would expect that the elevations of deltas increase with increasing distance from Chryse Planitia. This is obviously not the case, arguing against a formation by a regionally connected groundwater aquifer. The fact that the length of the contributing valleys appears to decrease with younger ages may suggest that the flow processes acted over longer times in the more distant past or that the water source may have been more regional for the older deltas, perhaps in the way envisaged by *Harrison and Grimm* [2005], who attributed valleys of this morphology and age to groundwater recharge (e.g., by basal melting of ice sheets), before smaller and younger valleys and deltas formed when a relatively thick cryosphere had already been in place [*Clifford et al.*, 2010].

[31] Delta morphology is diverse [*Hauber et al.*, 2009], and the observations of deltas described here for the first time (#9–15 in Figure 1 and Table 1) confirm earlier reports. For example, some of them display a very simple depositional architecture, such as the fan delta in an unnamed crater at 11.38°N/308.72°E (Figure 3; see also Figure 2d), while others are more complex and exhibit a geometry that is characteristic of Gilbert-type deltas (Figure 2b) [cf. *Hauber et al.*, 2009, Figure 6]. Two deltas display a long profile with distinct topographic steps (Figures 2a and 5a). Such "stepped" deltas were observed elsewhere on Mars (Figure 5b) and could be reproduced in the laboratory [*Kraal et al.*, 2008]. The stair-step topography of the deltas, in combination with the short-canyon lengths, is evidence for single-event energetic aqueous transport processes, characterized by a sudden release of water from subsurface water reservoirs, massive discharges, and short timescales [*Kraal et al.*, 2008; *Kleinhans et al.*, 2010]. Crater lake-delta modeling indicates that the amount of water involved is limited to the volume of the lake which formed in a short period, even accounting for evaporation and percolation. Such limited water volumes may have been provided by localized water supply from within the cryosphere (e.g., by melting). Therefore, no huge water volumes from widely dispersed sources such as precipitation appear to be required.

[32] The general lack of aqueous alteration minerals associated with the deltas is consistent with, but not diagnostic of, short formation times. Besides a dust cover, the most obvious explanation would be that water was simply not present long enough in these settings to enable their

formation. Even the few cases in which some alteration minerals were identified in Xanthe Terra and Aeolis Mensae do not indicate a sustained presence of water. The observation of opaline silica on two deltas supports scenarios of delta formation characterized by short formation times and generally dry conditions afterward. Again, these results appear to apply globally and are not restricted to the study areas around Chryse Planitia and in Nephentes and Aeolis Mensae [*Carter et al.*, 2012].

[33] The triggering mechanism for valley and delta formation is unclear. The older deltas with the longer contributing valleys may have formed as hypothesized by *Harrison and Grimm* [2005], who postulated an origin related to regional groundwater flow in response to decreasing surface runoff. Most valleys studied by *Harrison and Grimm* [2005] have a late Noachian and early Hesperian age, however, and the thickening cryosphere [*Clifford et al.*, 2010] would appear to preclude this mechanism for the younger deltas studied here. An impact-induced localized and transient climate favorable for precipitation [e.g., *Segura et al.*, 2012] seems to be ruled out in the Hesperian and Amazonian, since the required impacts are huge and would have occurred only rarely post-Noachian [*Toon et al.*, 2010]. Smaller impacts, however, could have provided thermal energy that perturbed the local cryospheric environment and produced a thermal disequilibrium, thus mobilizing meltwater. Mobilization of cryospheric ice by magmatism is a viable candidate mechanism, but Xanthe Terra does not exhibit evidence for significant post-Noachian volcanism (exceptions are few and far from the sources of valleys [*Hauber et al.*, 2012]). Intrusive magmatism, on the other hand, could be more widespread, and dikes have been unambiguously detected to the south of Xanthe Terra at the walls of Valles Marineris [*Flahaut et al.*, 2011]. No evidence for dikes, such as long and linear grabens, has been detected in Xanthe Terra though. Hot ejecta blankets from impacts or a transient climate episode may have triggered the fluvial activity producing the Eberswalde delta [*Mangold et al.*, 2012], and this mechanism is clearly a candidate for those valleys which originate on ejecta blankets (e.g., Subur Vallis). The positive correlation of valley length and delta ages (Figure 8c) may indicate an episodic valley formation, with some of the older and larger deltas (e.g., Sabrina, Tyras, Hypanis) representing the latest stage of activity associated with these valleys. In contrast, the younger deltas are linked to short and morphologically simple valleys that may have formed in one or few episodes only, reflecting the decreasing level of aqueous activity over time. Seismic energy from impacts or tectonic events may have also locally mobilized ice in the cryosphere, and neotectonic activity was indeed reported from chaotic regions around Chryse Planitia [*Spagnuolo et al.*, 2011]. Nevertheless, it remains an open question which or which combination of these candidate mechanisms was actually operating, and there may be other yet unidentified ways to form such deltas on Mars.

[34] Further age determination of Martian deltas can also be applied to address the question whether an ocean has existed on early Mars. It has been suggested that the elevations of deltas close to the highland/lowland dichotomy, which corresponds to the shorelines of a proposed ancient ocean, provide support for such an ocean covering the northern lowlands about 3.5 Gyr ago [*Di Achille and*

Hynek, 2010]. This hypothesis predicts an ocean with a shoreline at an elevation of −2540 m, and no delta would have formed below this global base level. Deltas delineating this contact should have about the same age as the ocean, and more thorough analysis (i.e., age dating and detailed morphologic analysis) of the deltas of *Di Achille and Hynek* [2010] would provide additional evidence to support or refute the global ocean hypothesis.

6. Conclusions

[35] 1. The formation of the deltas in our study areas around Chryse Planitia and in the Aeolis region occurred over a very long period of time, ranging from the early Hesperian to the late Amazonian. Similar ages were obtained for a set of morphologically analogous deltas in the eastern hemisphere, which were studied for comparison. It appears that our results are not restricted to a specific region, but are globally representative, and that similarly young deltas are widespread.

[36] 2. Valleys and associated deltas around Chryse Planitia and in Aeolis Mensae were formed by short-lived aqueous processes. The likely source of water was neither widespread precipitation nor a regionally connected groundwater aquifer, but water mobilized locally from the cryosphere, by one or a combination of several candidate trigger mechanisms.

[37] 3. The results of our study support the hypothesis that the formation of late-stage valleys and deltas did not require sustained periods of global climatic conditions favoring widespread precipitation.

[38] 4. The deltas are commonly not associated with aqueous alteration minerals. This may be partly caused by a dust cover, but it may also suggest that liquid water was never present long enough to enable their formation. The identification of opaline silica on two deltas further supports this notion, because opaline silica is easily transformed to other products by diagenesis.

[39] 5. The results obtained in this study show that liquid water has been locally present after the Noachian at the Martian surface, although only episodically, for transient intervals, and widely separated in space.

References

Aharonson, O., M. T. Zuber, D. H. Rothman, N. Schorghofer, and K. X. Whipple (2002), Drainage basins and channel incision on Mars, *Proc. Natl. Acad. Sci. U. S. A.*, 99, 1780–1783, doi:10.1073/pnas.261704198.

Anderson, J. H., and K. A. Wickersheim (1964), Near infrared characterization of water and hydroxyl groups on silica surfaces, *Surf. Sci.*, 2, 252–260.

Andrews-Hanna, J. C., and K. W. Lewis (2011), Early Mars hydrology: 2. Hydrological evolution in the Noachian and Hesperian epochs, *J. Geophys. Res.*, 116, E02007, doi:10.1029/2010JE003709.

Andrews-Hanna, J. C., and R. J. Phillips (2007), Hydrological modeling of outflow channels and chaos regions of Mars, *J. Geophys. Res.*, 112, E08001, doi:10.1029/2006JE002881.

Andrews-Hanna, J. C., R. J. Phillips, and M. T. Zuber (2007), Meridiani Planum and the global hydrology of Mars, *Nature*, *446*, 163–166, doi:10.1038/nature05594.

Ansan, V., et al. (2011), Stratigraphy, mineralogy, and origin of layered deposits inside Terby crater, Mars, *Icarus*, *211*, 273–304, doi:10.1016/j.icarus.2010.09.011.

Baker, V. R. (2001), Water and the Martian landscape, *Nature*, *412*, 228–236, doi:10.1038/35084172.

Baker, V. R., and D. J. Milton (1974), Erosion by catastrophic floods on Mars and Earth, *Icarus*, *23*, 27–41, doi:10.1016/0019-1035(74)90101-8.

Baker, V. R., R. G. Strom, V. C. Gulick, J. S. Kargel, G. Komatsu, and V. S. Kale (1991), Ancient oceans, ice sheets, and the hydrological cycle on Mars, *Nature*, *354*, 86–87, doi:10.1038/354086a0.

Barabash, S., A. Fedorov, R. Lundin, and J.-A. Sauvaud (2007), Martian atmospheric erosion rates, *Science*, *315*, 501–503, doi:10.1126/science.1134358.

Barnhart, C. J., A. D. Howard, and J. M. Moore (2009), Long-term precipitation and late-stage valley network formation: Landform simulations of Parana Basin, Mars, *J. Geophys. Res.*, *114*, E01003, doi:10.1029/2008JE003122.

Bibring, J.-P., Y. Langevin, J. F. Mustard, F. Poulet, R. Arvidson, A. Gendrin, B. Gondet, N. Mangold, and the OMEGA Team (2006), Global mineralogical and aqueous Mars history derived from OMEGA/Mars Express data, *Science*, *312*, 400–404, doi:10.1126/science.1122659.

Blair, T. C., and J. G. McPherson (2009), Processes and forms of alluvial fans, in *Geomorphology of Desert Environments*, 2nd ed., edited by A. J. Parsons, and A. D. Abrahams, pp. 413–467, Springer, Netherlands, doi:10.1007/978-1-4020-5719-9_14.

Cabrol, N. A., and E. A. Grin (2001), The evolution of lacustrine environments on Mars: Is Mars only hydrologically dormant?, *Icarus*, *149*, 291–328, doi:10.1006/icar.2000.6530.

Carr, M. H. (1979), Formation of Martian flood features by release of water from confined aquifers, *J. Geophys. Res.*, *84*, 2995–3007, doi:10.1029/JB084iB06p02995.

Carr, M. H. (2012), The fluvial history of Mars, *Philos. Trans. R. Soc. A*, *370*, 2193–2215, doi:10.1098/rsta.2011.0500.

Carter, J., F. Poulet, N. Mangold, V. Ansan, E. Dehouck, J.-P. Bibring, and S. Murchie (2012), Composition of alluvial fans and deltas on Mars, 43rd Lunar and Planet, Sci. Con., Abstract 1978.

Carter, J., F. Poulet, J.-P. Bibring, N. Mangold, and S. Murchie (2013), Hydrous minerals on Mars as seen by the CRISM and OMEGA imaging spectrometers: Updated global view, *J. Geophys. Res. Planets*, *118*, 831–858, doi:10.1029/2012JE004145.

Christensen, P. R. (2003), Formation of recent Martian gullies through melting of extensive water-rich snow deposits, *Nature*, *422*, 45–48, doi:10.1038/nature01436.

Clark, R. N., G. A. Swayze, R. Wise, E. Livo, T. Hoefen, R. Kokaly, and S. J. Sutley (2007), USGS digital spectral library splib06a: U.S. Geological Survey, Digital Data Series 231. [Available at http://speclab.cr.usgs.gov/spectral.lib06].

Clifford, S. M. (1993), A model for the hydrologic and climatic behavior of water on Mars, *J. Geophys. Res.*, *98*, 10,973–11,016, doi:10.1029/93JE00225.

Clifford, S. M., J. Lasue, E. Heggy, J. Boisson, P. McGovern, and M. D. Max (2010), Depth of the Martian cryosphere: Revised estimates and implications for the existence and detection of subpermafrost groundwater, *J. Geophys. Res.*, *115*, E07001, doi:10.1029/2009JE003462.

Costard, F., F. Forget, N. Mangold, and J. P. Peulvast (2002), Formation of recent Martian debris flows by melting of near-surface ground ice at high obliquity, *Science*, *295*, 110–113, doi:10.1126/science.1066698.

Craddock, R. A., and A. D. Howard (2002), The case for rainfall on a warm, wet early Mars, *J. Geophys. Res.*, *107*(E11), 5111, doi:10.1029/2001JE001505.

Craddock, R. A., and T. A. Maxwell (1993), Geomorphic evolution of the Martian highlands through ancient fluvial processes, *J. Geophys. Res.*, *98*, 3453–3468, doi:10.1029/92JE02508.

Craddock, R. A., T. A. Maxwell, and A. D. Howard (1997), Crater morphometry and modification in the Sinus Sabaeus and Margaritifer Sinus regions of Mars, *J. Geophys. Res.*, *102*, 13,321–13,340, doi:10.1029/97JE01084.

Dehouck, E., N. Mangold, S. Le Mouélic, V. Ansan, and F. Poulet (2010), Ismenius Cavus, Mars: A deep paleolake with phyllosilicate deposits, *Planet. Space Sci.*, *58*, 941–946, doi:10.1016/j.pss.2010.02.005.

Di Achille, G., and B. M. Hynek (2010), Ancient ocean on Mars supported by global distribution of deltas and valleys, *Nat. Geosci.*, *3*, 459–463, doi:10.1038/ngeo891.

Di Achille, G., G.-G. Ori, and D. Reiss (2007), Evidence for late Hesperian lacustrine activity in Shalbatana Vallis, Mars, *J. Geophys. Res.*, *112*, E07007, doi:10.1029/2006JE002858.

Dickson, J. L., and J. W. Head (2009), The formation and evolution of youthful gullies on Mars: Gullies as the late-stage phase of Mars' most recent ice age, *Icarus*, *204*, 63–86, doi:10.1016/j.icarus.2009.06.018.

Dundas, C. M., S. Diniega, C. J. Hansen, S. Byrne, and A. S. McEwen (2012), Seasonal activity and morphological changes in Martian gullies, *Icarus*, *220*, 124–143, doi:10.1016/j.icarus.2012.04.005.

Ehlmann, B. L., G. Berger, N. Mangold, J. R. Michalski, D. C. Catling, S. W. Ruff, E. Chassefière, P. B. Niles, V. Chevrier, and F. Poulet (2013), Geochemical consequences of widespread clay mineral formation in Mars' ancient crust, *Space Sci. Rev.*, *174*, 329–364, doi:10.1007/s11214-012-9930-0.

Erkeling, G., D. Reiss, H. Hiesinger, and R. Jaumann (2010), Morphologic, stratigraphic and morphometric investigations of valley networks in eastern Libya Montes, Mars: Implications for the Noachian/Hesperian climate change, *Earth Planet. Sci. Lett.*, *294*, 291–305.

Fassett, C. I., and J. W. Head (2005), Fluvial sedimentary deposits on Mars: Ancient deltas in a crater lake in the Nili Fossae region, *Geophys. Res. Lett.*, *32*, L14201, doi:10.1029/2005GL023456.

Fassett, C. I., and J. W. Head (2007), Valley formation on Martian volcanoes in the Hesperian: Evidence for melting of summit snowpack, caldera lake formation, drainage and erosion on Ceraunius Tholus, *Icarus*, *189*, 118–135, doi:10.1016/j.icarus.2006.12.021.

Fassett, C. I., and J. W. Head (2008a), The timing of Martian valley network activity: Constraints from buffered crater counting, *Icarus*, *195*, 61–89, doi:10.1016/j.icarus.2007.12.009.

Fassett, C. I., and J. W. Head (2008b), Valley network-fed, open-basin lakes on Mars: Distribution and implications for Noachian surface and subsurface hydrology, *Icarus*, *198*, 37–56, doi:10.1016/j.icarus.2008.06.016.

Fassett, C. I., J. L. Dickson, J. W. Head, J. S. Levy, and D. R. Marchant (2010), Supraglacial and proglacial valleys on Amazonian Mars, *Icarus*, *208*, 86–100, doi:10.1016/j.icarus.2010.02.021.

Flahaut, J., J. F. Mustard, C. Quantin, H. Clenet, P. Allemand, and P. Thomas (2011), Dikes of distinct composition intruded into Noachian-aged crust exposed in the walls of Valles Marineris, *Geophys. Res. Lett.*, *38*, L15202, doi:10.1029/2011GL048109.

Frey, H. (2008), Ages of very large impact basins on Mars: Implications for the late heavy bombardment in the inner solar system, *Geophys. Res. Lett.*, *35*, L13203, doi:10.1029/2008GL033515.

Garvin, J. B., S. E. H. Sakimoto, and J. J. Frawley (2003), Craters on Mars: Global geometric properties from gridded MOLA topography, Sixth International Conference on Mars, Abstract #3277.

Gendrin, A., et al. (2005), Sulfates in Martian layered terrains: The OMEGA/Mars Express view, *Science*, *307*, 1587–1591, doi:10.1126/science.1109087.

Gilbert, G. K. (1885), The topographic features of lake shores, *U.S. Geol. Surv. Annu. Rep.*, *5*, 75–123.

Goldspiel, J. M., and S. W. Squyres (2000), Groundwater sapping and valley formation on Mars, *Icarus*, *148*, 176–192, doi:10.1006/icar.2000.6465.

Golombek, M. P., et al. (2006), Erosion rates at the Mars Exploration Rover landing sites and long-term climate change on Mars, *J. Geophys. Res.*, *111*, E12S10, doi:10.1029/2006JE002754.

Goudge, T. A., J. W. Head, J. F. Mustard, and C. I. Fassett (2012a), An analysis of open-basin lake deposits on Mars: Evidence for the nature of associated lacustrine deposits and post-lacustrine modification processes, *Icarus*, *219*, 211–229, doi:10.1016/j.icarus.2012.02.027.

Goudge, T. A., J. F. Mustard, J. W. Head, and C. I. Fassett (2012b), Constraints on the history of open-basin lakes on Mars from the composition and timing of volcanic resurfacing, *J. Geophys. Res.*, *117*, E00J21, doi:10.1029/2012JE004115.

Grant, J. A., and T. Parker (2002), Drainage evolution in the Margaritifer Sinus region, Mars, *J. Geophys. Res.*, *107*(E9), 5066, doi:10.1029/2001JE001678.

Grant, J. A., and S. A. Wilson (2011), Late alluvial fan formation in southern MargaritiferTerra, Mars, *Geophys. Res. Lett.*, *38*, L08201, doi:10.1029/2011GL046844.

Grant, J. A., and S. A. Wilson (2012), A possible synoptic source of water for alluvial fan formation in southern Margaritifer Terra, Mars, *Planet. Space Sci.*, *72*, 44–52, doi:10.1016/j.pss.2012.05.020.

Gulick, V. C., and V. R. Baker (1990), Origin and evolution of valleys on Martian volcanoes, *J. Geophys. Res.*, *95*, 14,325–14,344, doi:10.1029/JB095iB09p14325.

Gwinner, K., F. Scholten, F. Preusker, S. Elgner, T. Roatsch, M. Spiegel, R. Schmidt, J. Oberst, R. Jaumann, and C. Heipke (2010), Topography of Mars from global mapping by HRSC high-resolution digital terrain 2 models and orthoimages: Characteristics and performance, *Earth Planet. Sci. Lett.*, *294*, 506–519, doi:10.1016/j.epsl.2009.11.007.

Hanna, J. C., and R. J. Phillips (2005), Hydrological modeling of the Martian crust with application to the pressurization of aquifers, *J. Geophys. Res.*, *110*, E01004, doi:10.1029/2004JE002330.

Harrison, K. P., and R. E. Grimm (2005), Groundwater-controlled valley networks and the decline of surface runoff on early Mars, *J. Geophys. Res.*, *110*, E12S16, doi:10.1029/2005JE002455.

Harrison, K. P., and R. E. Grimm (2009), Regionally compartmented groundwater flow on Mars, *J. Geophys. Res.*, *114*, E04004, doi:10.1029/2008JE003300.

Hartmann, W. K., and G. Neukum (2001), Cratering chronology and the evolution of Mars, *Space Sci. Rev.*, *96*, 165–194, doi:10.1023/A:1011945222010.

Hauber, E., K. Gwinner, M. Kleinhans, D. Reiss, G. Di Achille, G.-G. Ori, F. Scholten, L. Marinangeli, R. Jaumann, and G. Neukum (2009), Sedimentary deposits in Xanthe Terra: Implications for the ancient climate on Mars, *Planet. Space Sci.*, *57*, 944–957, doi:10.1016/j.pss.2008.06.009.

Hauber, E., et al. (2011), Landscape evolution in Martian mid-latitude regions: Insights from analogous periglacial landforms in Svalbard, in *Martian Geomorphology*, Geological Society, Special Publications, vol. 356, edited by M. R. Balme et al., pp. 111–131, Geological Society, London.

Hauber, E., T. Platz, M. Kleinhans, L. Le Deit, P. Carbonneau, T. De Haas, W. Marra, and D. Reiss (2012), Old or not so old: That is the question for deltas and fans in Xanthe Terra, Mars, Third Conference on Early Mars: Geologic, Hydrologic, and Climatic Evolution and the Implications for Life, LPI Contribution No. 1680, Abstract #7078.

Head, J. W., L. Wilson, and K. L. Mitchell (2003), Generation of recent massive water floods at Cerberus Fossae, Mars, by dike emplacement, cryosphere cracking, and confined aquifer groundwater release, *Geophys. Res. Lett.*, *30*(11), 1577, doi:10.1029/2003GL017135.

Hoke, M. R. T., and B. M. Hynek (2009), Roaming zones of precipitation on ancient Mars as recorded in valley networks, *J. Geophys. Res.*, *114*, E08002, doi:10.1029/2008JE003247.

Howard, A. D., and J. M. Moore (2011), Late Hesperian to early Amazonian midlatitude Martian valleys: Evidence from Newton and Gorgonum basins, *J. Geophys. Res.*, *116*, E05003, doi:10.1029/2010JE003782.

Howard, A. D., R. C. Kochel, and H. R. Holt (Eds.) (1988), *Sapping Features of the Colorado Plateau—A comparative planetary geology field guide*, NASA SP-491, Washington, DC.

Howard, A. D., J. M. Moore, and R. P. Irwin (2005), An intense terminal epoch of widespread fluvial activity on early Mars: 1. Valley network incision and associated deposits, *J. Geophys. Res.*, *110*, E12S14, doi:10.1029/2005JE002459.

Hynek, B. M., M. Beach, and M. R. T. Hoke (2010), Updated global map of Martian valley networks and implications for climate and hydrologic processes, *J. Geophys. Res.*, *115*, E09008, doi:10.1029/2009JE003548.

Irwin, R. P., and T. R. Watters (2010), Geology of the Martian crustal dichotomy boundary: Age, modifications, and implications for modeling efforts, *J. Geophys. Res.*, *115*, E11006, doi:10.1029/2010JE003658.

Irwin, R. P., T. R. Watters, A. D. Howard, and J. R. Zimbelman (2004), Sedimentary resurfacing and fretted terrain development along the crustal dichotomy boundary, Aeolis Mensae, Mars, *J. Geophys. Res.*, *109*, E09011, doi:10.1029/2004JE002248.

Irwin, R. P., A. D. Howard, R. A. Craddock, and J. M. Moore (2005), An intense terminal epoch of widespread fluvial activity on early Mars: 2. Increased runoff and paleolake development, *J. Geophys. Res.*, *110*, E12S15, doi:10.1029/2005JE002460.

Irwin, R. P., A. D. Howard, and R. A. Craddock (2008), Fluvial valley networks on Mars, in *River Confluences, Tributaries, and the Fluvial Network*, edited by S. P. Rice, et al., pp. 419–451, Wiley, Chichester, U.K.

Ivanov, B. A. (2001), Mars/Moon cratering ratio estimates, *Space Sci. Rev.*, *96*, 87–104, doi:10.1023/A:1011941121102.

Jaumann, R., et al. (2007), The High Resolution Stereo Camera (HRSC) experiment on Mars Express: Instrument aspects and experiment conduct from interplanetary cruise through the nominal mission, *Planet. Space Sci.*, *55*, 928–952, doi:10.1016/j.pss.2006.12.003.

Kleinhans, M. G., H. E. van de Kasteele, and E. Hauber (2010), Palaeoflow reconstruction from fan delta morphology on Mars, *Earth Planet. Sci. Lett.*, *294*, 378–392, doi:10.1016/j.epsl.2009.11.025.

Kneissl, T., S. van Gasselt, and G. Neukum (2011), Map-projection-independent crater size-frequency determination in GIS environments—New software tool for ArcGIS, *Planet. Space Sci.*, *59*, 1243–1254, doi:10.1016/j.pss.2010.03.015.

Kraal, E. R., M. van Dijk, G. Postma, and M. G. Kleinhans (2008), Martian stepped-delta formation by rapid water release, *Nature*, *451*, 973–976, doi:10.1038/nature06615.

Laity, J. E., and M. C. Malin (1985), Sapping processes and the development of theater-headed valley networks on the Colorado Plateau, *Geol. Soc. Am. Bull.*, *96*, 203–217.

Lamb, M. P., A. D. Howard, J. Johnson, K. X. Whipple, W. E. Dietrich, and J. T. Perron (2006), Can springs cut canyons into rock?, *J. Geophys. Res.*, *111*, E07002, doi:10.1029/2005JE002663.

Lamb, M. P., W. E. Dietrich, S. M. Aciego, D. J. DePaolo, and M. Manga (2008), Formation of Box Canyon, Idaho, by megaflood: Implications for seepage erosion on Earth and Mars, *Science*, *320*, 1067–1070, doi:10.1126/science.1156630.

Lammer, H., et al. (2013), Outgassing history and escape of the Martian atmosphere and water inventory, *Space Sci. Rev.*, *174*, 113–154, doi:10.1007/s11214-012-9943-8.

Lasue, J., N. Mangold, E. Hauber, S. Clifford, W. Feldman, O. Gasnault, C. Grima, S. Maurice, and O. Mousis (2013), Quantitative assessments of the Martian hydrosphere, *Space Sci. Rev.*, *174*, 155–212, doi:10.1007/s11214-012-9946-5.

Le Deit, L., J. Flahaut, C. Quantin, E. Hauber, D. Mége, O. Bourgeois, J. Gurgurewicz, M. Massé, and R. Jaumann (2012), Extensive surface pedogenic alteration of the Martian Noachian crust suggested by plateau phyllosilicates around Valles Marineris, *J. Geophys. Res.*, *117*, E00J05, doi:10.1029/2011JE003983.

Luo, W., and A. D. Howard (2008), Computer simulation of the role of groundwater seepage in forming Martian valley networks, *J. Geophys. Res.*, *113*, E05002, doi:10.1029/2007JE002981.

Luo, W., and T. F. Stepinski (2006), Topographically derived maps of valley networks and drainage density in the Mare Tyrrhenum quadrangle of Mars, *Geophys. Res. Lett.*, *33*, L18202, doi:10.1029/2006GL027346.

Luo, W., R. E. Arvidson, M. Sultan, R. Becker, M. K. Crombie, N. Sturchio, and Z. E. Alfy (1997), Groundwater sapping processes, Western Desert, Egypt, *Geol. Soc. Am. Bull.*, *109*, 43–62, doi:10.1130/0016-7606(1997)109<0043:GWSPWD>2.3.CO;2.

Malin, M. C., and K. S. Edgett (2000), Evidence for recent groundwater seepage and surface runoff on Mars, *Science*, *288*(5475), 2330–2335, doi:10.1126/science.288.5475.2330.

Malin, M. C., G. E. Danielson, A. P. Ingersoll, H. Masursky, J. Veverka, M. A. Ravine, and T. A. Soulanille (1992), Mars Observer Camera, *J. Geophys. Res.*, *97*, 7699–7718, doi:10.1029/92JE00340.

Malin, M. C., et al. (2007), Context camera investigation on board the Mars Reconnaissance Orbiter, *J. Geophys. Res.*, *112*, E05S04, doi:10.1029/2006JE002808.

Mangold, N., C. Quantin, V. Ansan, C. Delacourt, and P. Allemand (2004), Evidence for precipitation on Mars from dendritic valleys in the Valles Marineris area, *Science*, *305*, 78–81, doi:10.1126/science.1097549.

Mangold, N., et al. (2007), Mineralogy of the Nili Fossae region with OMEGA/MarsExpress data: 2. Aqueous alteration of the crust, *J. Geophys. Res.*, *112*, E08S04, doi:10.1029/2006JE002835.

Mangold, N., E. S. Kite, M. G. Kleinhans, H. Newsom, V. Ansan, E. Hauber, E. Kraal, C. Quantin, and K. Tanaka (2012), The origin and timing of fluvial activity at Eberswalde crater, Mars, *Icarus*, *220*, 530–551, doi:10.1016/j.icarus.2012.05.026.

McEwen, A. S., et al. (2007), Mars Reconnaissance Orbiter's High Resolution Imaging Science Experiment (HiRISE), *J. Geophys. Res.*, *112*, E05S02, doi:10.1029/2005JE002605.

McEwen, A. S., L. Ojha, C. M. Dundas, S. S. Mattson, S. Byrne, J. J. Wray, S. C. Cull, S. L. Murchie, N. Thomas, and V. C. Gulick (2011), Seasonal flows on warm Martian slopes, *Science*, *333*, 740–743, doi:10.1126/science.1204816.

McLennan, S. M. (2003), Sedimentary silica on Mars, *Geology*, *31*, 315–318, doi:10.1130/0091-7613(2003)031<0315:SSOM>2.0.CO;2.

Michael, G. G. (2013), Planetary surface dating from crater size-frequency distribution measurements: Differential presentation of data for resurfaced units, Lunar Planet. Sci. Conf., 44, abstract #2181.

Michael, G. G., and G. Neukum (2010), Planetary surface dating from crater size-frequency distribution measurements: Partial resurfacing events and statistical age uncertainty, *Earth Planet. Sci. Lett.*, *294*, 223–229, doi:10.1016/j.epsl.2009.12.041.

Michael, G. G., T. Platz, T. Kneissl, and N. Schmedemann (2012), Planetary surface dating from crater size-frequency distribution measurements: Spatial randomness and clustering, *Icarus*, *218*, 169–177, doi:10.1016/j.icarus.2011.11.033.

Michalski, J. R., J. Cuadros, P. B. Niles, J. Parnell, A. D. Rogers, and S. P. Wright (2013), Groundwater activity on Mars and implications for a deep biosphere, *Nat. Geosci.*, *6*, 133–138, doi:10.1038/ngeo1706.

Milliken, R. E., et al. (2008), Opaline silica in young deposits on Mars, *Geology*, *36*, 847–850, doi:10.1130/G24967A.1.

Möhlmann, D., and K. Thomsen (2011), Properties of cryobrines on Mars, *Icarus*, *212*, 123–130, doi:10.1016/j.icarus.2010.11.025.

Moore, J. M., and A. D. Howard (2005), Large alluvial fans on Mars, *J. Geophys. Res.*, *110*, E04005, doi:10.1029/2004JE002352.

Murchie, S. L., et al. (2009), The compact reconnaissance imaging spectrometer for Mars investigation and data set from the Mars Reconnaissance Orbiter's primary science phase, *J. Geophys. Res.*, *114*, E00D07, doi:10.1029/2009JE003344.

Nichols, G. (2009), *Sedimentology and Stratigraphy*, 2nd ed., 419 pp., Wiley-Blackwell, Chichester, UK.

Noe Dobrea, E. Z., J. F. Bell, T. H. McConnochie, and M. Malin (2006), Analysis of a spectrally unique deposit in the dissected Noachian terrain of Mars, *J. Geophys. Res.*, *111*, E06007, doi:10.1029/2005JE002431.

Penido, J. C., C. I. Fassett, and S. M. Som (2013), Scaling relationships and concavity of small valley networks on Mars, *Planet. Space Sci.*, *75*, 105–116, doi:10.1016/j.pss.2012.09.009.

Pieri, D. C. (1980), Martian valleys: Morphology, distribution, age, and origin, *Science*, *210*, 895–897, doi:10.1126/science.210.4472.895.

Platz, T., G. G. Michael, K. L. Tanaka, J. A. Skinner, and C. M. Fortezzo (2013), Crater-based dating of geological units on Mars: Methods and application for the new global geological map, *Icarus*, *225*, 806–827, doi:10.1016/j.icarus.2013.04.021.

Pondrelli, M., A. P. Rossi, L. Marinangeli, E. Hauber, K. Gwinner, A. Baliva, and S. di Lorenzo (2008), Evolution and depositional environments of the Eberswalde fan delta, Mars, *Icarus*, *197*, 429–451, doi:10.1016/j.icarus.2008.05.018.

Popa, C., F. Esposito, and L. Colangeli (2010), New landing site proposal for Mars Science Laboratory (MSL) in Xanthe Terra, Lunar Planet. Sci., XLI, Abstract #1807.

Poulet, F., J.-P. Bibring, J. F. Mustard, A. Gendrin, N. Mangold, Y. Langevin, R. E. Arvidson, B. Gondet, C. Gomez, and the OMEGA Team (2005), Phyllosilicates on Mars and implications for early Martian climate, *Nature*, *438*, 623–627, doi:10.1038/nature04274.

Reiss, D., S. van Gasselt, G. Neukum, and R. Jaumann (2004), Absolute dune ages and implications for the time of formation of gullies in Nirgal Vallis, Mars, *J. Geophys. Res.*, *109*, E06007, doi:10.1029/2004JE002251.

Reiss, D., H. Hiesinger, E. Hauber, and K. Gwinner (2009), Regional differences in gully occurrence on Mars: A comparison between the Hale and Bond craters, *Planet. Space Sci.*, *57*, 958–974, doi:10.1016/j.pss.2008.09.008.

Reiss, D., G. Erkeling, K. E. Bauch, and H. Hiesinger (2010), Evidence for present day gully activity on the Russell crater dune field, Mars, *Geophys. Res. Lett.*, *37*, L06203, doi:10.1029/2009GL042192.

Rotto, S., and K. L. Tanaka (1995), Geologic/geomorphic map of the Chryse Planitia region of Mars, US Geological Survey Misc. Invest. Series Map I-2441, scale 1:5,000,000.

Ruff, S. W., and P. R. Christensen (2002), Bright and dark regions on Mars: Particle size and mineralogical characteristics based on Thermal Emission Spectrometer data, *J. Geophys. Res.*, *107*(E12), 5127, doi:10.1029/2001JE001580.

Scholten, F., K. Gwinner, T. Roatsch, K.-D. Matz, M. Wählisch, B. Giese, J. Oberst, R. Jaumann, G. Neukum, and the HRSC Co-Investigator Team (2005), Mars Express HRSC data processing—Methods and operational aspects, *Photogramm. Eng. Remote Sens.*, *71*, 1143–1152.

Schon, S. C., J. W. Head, and C. I. Fassett (2009), Unique chrono-stratigraphic marker in depositional fan stratigraphy on Mars: Evidence for ca. 1.25 Ma gully activity and surficial meltwater origin, *Geology*, *37*, 207–210, doi:10.1130/G25398A.1.

Segura, T. L., C. P. McKay, and O. B. Toon (2012), An impact-induced, stable, runaway climate on Mars, *Icarus*, *220*, 144–148, doi:10.1016/j.icarus.2012.04.013.

Sharp, R. P. (1973), Mars: Fretted and chaotic terrains, *J. Geophys. Res.*, *78*, 4073–4083, doi:10.1029/JB078i020p04073.

Spagnuolo, M., A. P. Rossi, E. Hauber, and S. van Gasselt (2011), Recent tectonics and subsidence on Mars: Hints from Aureum Chaos, *Earth Planet. Sci. Lett.*, *312*, 13–21, doi:10.1016/j.epsl.2011.09.052.

Stepinski, T. F., and S. Coradetti (2004), Comparing morphologies of drainage basins on Mars and Earth using integral-geometry and neural maps, *Geophys. Res. Lett.*, *31*, L15604, doi:10.1029/2004GL020359.

Tanaka, K. L., J. A. Skinner, and T. M. Hare (2005), Geologic map of the northern plains of Mars, U.S. Geol. Survey, Scientific Investigations Map 2888, scale 1:15,000,000.

Toon, O. B., T. Segura, and K. Zahnle (2010), The formation of Martian river valleys by impacts, *Annu. Rev. Earth Planet. Sci.*, *38*, 303–322, doi:10.1146/annurev-earth-040809-152354.

Tosca, N. J., and A. H. Knoll (2009), Juvenile chemical sediments and the long-term persistence of water at the surface of Mars, *Earth Planet. Sci. Lett.*, *286*, 379–386, doi:10.1016/j.epsl.2009.07.004.

de Villiers, G., M. G. Kleinhans, and G. Postma (2013), Experimental delta formation in crater lakes and implications for interpretation of Martian deltas, *J. Geophys. Res. Planets*, *118*, 651–670, doi:10.1002/jgre.20069.

Warner, N., S. Gupta, J.-P. Muller, J.-R. Kim, and S.-Y. Lin (2009), A refined chronology of catastrophic outflow events in Ares Vallis, Mars, *Earth Planet. Sci. Lett.*, *288*, 58–69, doi:10.1016/j.epsl.2009.09.008.

Werner, S. C., and K. L. Tanaka (2011), Redefinition of the crater-density and absolute-age boundaries for the chronostratigraphic system of Mars, *Icarus*, *215*, 603–607, doi:10.1016/j.icarus.2011.07.024.

Williams, L. A., and D. A. Crerar (1985), Silica diagenesis, II. General mechanisms, *J. Sediment. Petrol.*, *55*, 312–321, doi:10.1306/212F86B1-2B24-11D7-8648000102C1865D.

Williams, L. A., G. A. Parks, and D. A. Crerar (1985), Silica diagenesis, I. Solubility controls, *J. Sediment. Petrol.*, *55*, 301–311, doi:10.1306/212F86AC-2B24-11D7-8648000102C1865D.

Williams, K. E., O. B. Toon, J. L. Heldmann, and M. T. Mellon (2009), Ancient melting of mid-latitude snowpacks on Mars as a water source for gullies, *Icarus*, *200*, 418–425, doi:10.1016/j.icarus.2008.12.013.

Williams, R. M. E., D. A. Rogers, M. Chojnacki, J. Boyce, K. D. Seelos, C. Hardgrove, and F. Chuang (2011), Evidence for episodic alluvial fan formation in far western Terra Tyrrhena, Mars, *Icarus*, *211*, 222–237, doi:10.1016/j.icarus.2010.10.001.

Wilson, L., and J. W. Head (2004), Evidence for a massive phreatomagmatic eruption in the initial stages of formation of the Mangala Valles outflow channel, Mars, *Geophys. Res. Lett.*, *31*, L15701, doi:10.1029/2004GL020322.

Wood, L. J. (2006), Quantitative geomorphology of the Mars Eberswalde delta, *Geol. Soc. Am. Bull.*, *118*, 557–566, doi:10.1130/B25822.1.

Zuber, M. T., D. E. Smith, S. C. Solomon, D. O. Muhleman, J. W. Head, J. B. Garvin, J. B. Abshire, and J. L. Bufton (1992), The Mars Observer laser altimeter investigation, *J. Geophys. Res.*, *97*, 7781–7797, doi:10.1029/92JE00341.